Cell Reports, Volume *18*

Supplemental Information

EBI2 Is Highly Expressed in Multiple Sclerosis Lesions and Promotes Early CNS Migration of Encephalitogenic CD4 T Cells

Florian Wanke, Sonja Moos, Andrew L. Croxford, André P. Heinen, Stephanie Gräf, Bettina Kalt, Denise Tischner, Juan Zhang, Isabelle Christen, Julia Bruttger, Nir Yogev, Yilang Tang, Morad Zayoud, Nicole Israel, Khalad Karram, Sonja Reißig, Sonja M. Lacher, Christian Reichhold, Ilgiz A. Mufazalov, Avraham Ben-Nun, Tanja Kuhlmann, Nina Wettschureck, Andreas W. Sailer, Klaus Rajewsky, Stefano Casola, Ari Waisman, and Florian C. Kurschus

Supplementary Figures

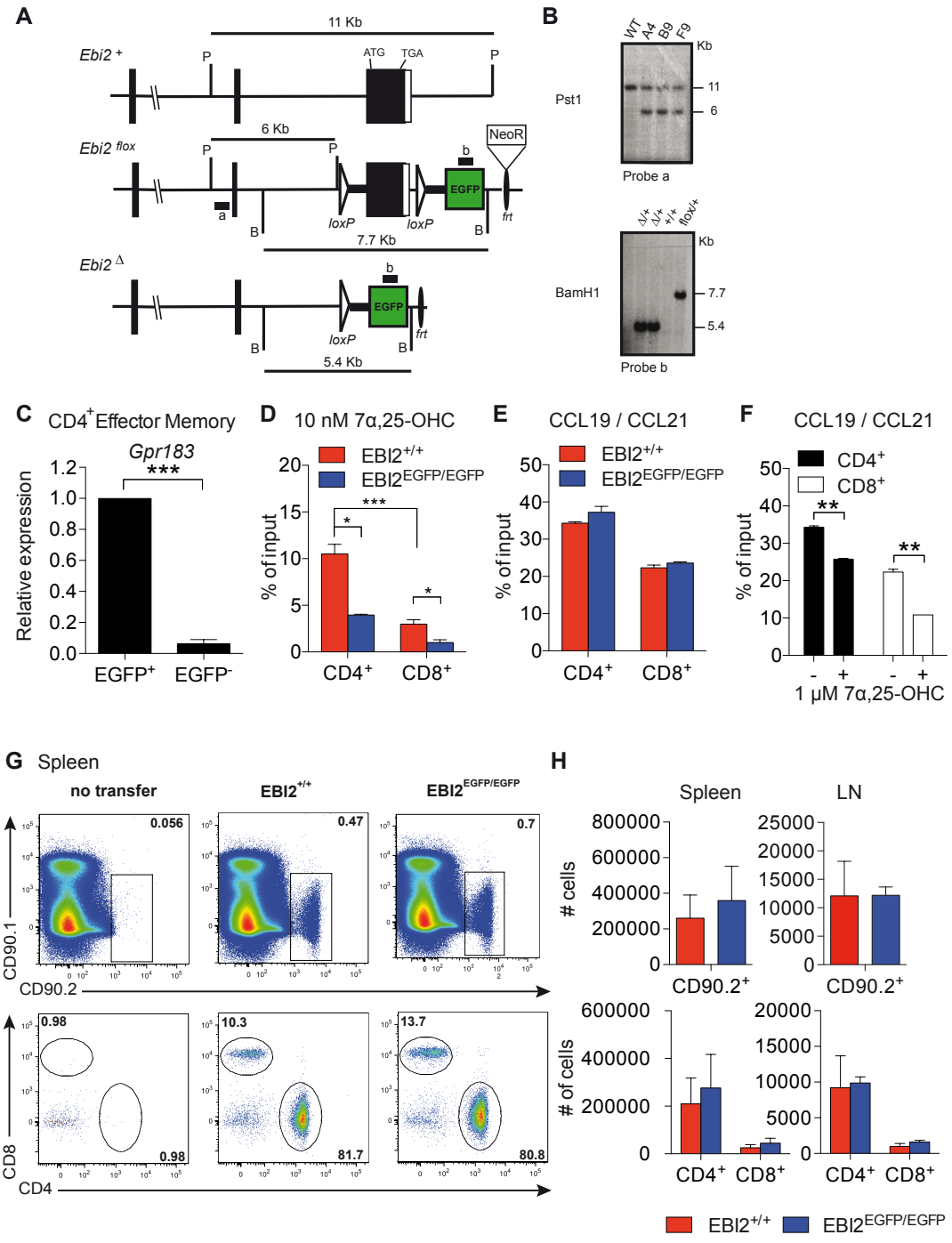

Figure S1. Related to Figure 1. Generation and characterization of *EBI2*^{EGFP} mice. (A) Conditional gene targeting strategy to generate conditional EBI2 knockout (EBI2^{fl}) mice. The single EBI2 coding exon is flanked by loxP sites. The intronic region that precedes the EBI2 coding exon, belonging to the floxed segment, was cloned upstream of an EGFP reporter cassette, which was finally placed downstream of the *EBI2*^{fl} DNA segment. Upon Cre-mediated recombination, the coding exon of *EBI2* is replaced by the EGFP minigene, generating a chimeric *EBI2-EGFP* allele that fails to express EBI2 (Ebi2$^{\Delta}$). The neomycin resistance gene flanked by FRT sites was eliminated *in vivo* crossing EBI2^{fl} mice to the FLPe deleter strain. (B) Correct targeting of ES clones was proofed by Southern blotting analysis using probes indicated (a and b). *In vivo* Cre-mediated recombination of the Ebi2^{fl} allele was confirmed by Southern blotting. (C) Relative expression of *Gpr183* mRNA of FACS-sorted EGFP^{+} and EGFP^{-} CD4^{+} effector memory T cells (CD62L^{-} / CD44^{+}). Value for EGFP^{+} cells was

considered as 1 to compare expression of EGFP$^-$ cells. Data is representative for two independent experiments. (D) Migration of purified pre-activated CD4$^+$ and CD8$^+$ T cells towards 10 nM 7α,25-OHC. Data is representative for two independent experiments. (E) Migration of purified and pre-activated CD4$^+$ and CD8$^+$ T cells towards 50 ng/ml CCL19 and CCL21. Data is representative for two independent experiments. (F) Migration of purified and pre-activated CD4$^+$ and CD8$^+$ T cells in the presence or absence of 1 µM 7α,25-OHC towards 50 ng/ml CCL19 and CCL21. Data is representative of at least two independent experiments. (G-H) EBI2 deficient T cells show normal homing to peripheral lymphoid organs. T cells were purified from either EBI2$^{EGFP/EGFP}$ mice or littermate controls and transferred i.v. into congenic host mice. Four hours later, cells in the spleen and lymph nodes were analyzed and quantified via flow cytometry. Transferred T cells were determined as living CD90.1$^-$ / CD90.2$^+$ T cells. (G) Flow cytometric analysis of transferred T cells in the spleen of recipient mice. (H) Quantification of transferred T cells from either EBI2$^{EGFP/EGFP}$ mice or littermate controls in the spleen (left) of lymph nodes (right) of recipient mice. Data is representative for two independent experiments (n=5).

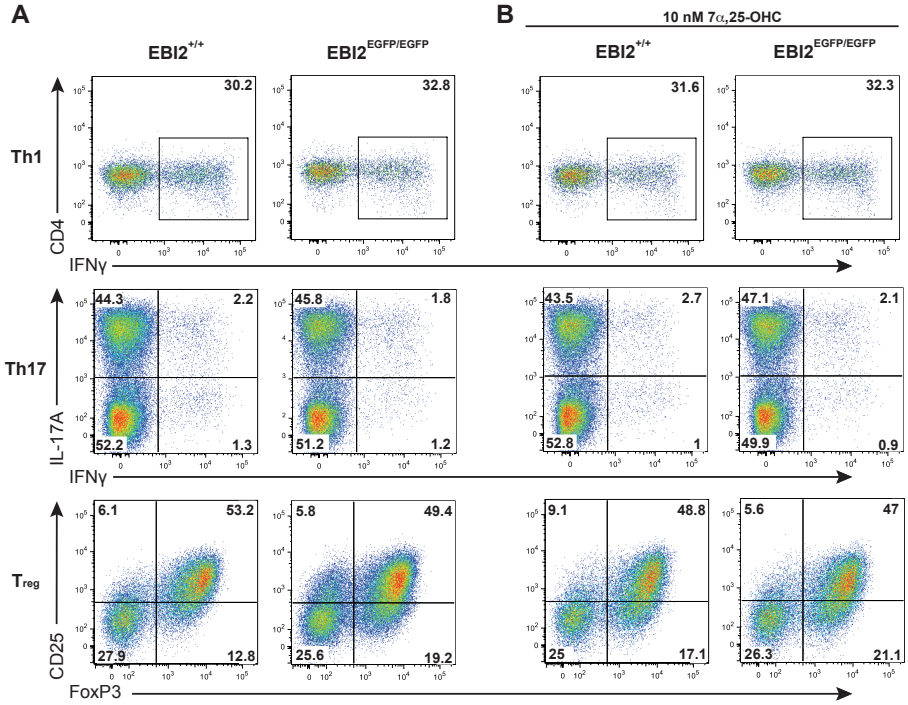

Figure S2. Related to Figure 2. (A-B) Cytokine and FoxP3 expression of *in vitro* differentiated naïve CD4$^+$ T cells from EBI2$^{+/+}$ and EBI2$^{EGFP/EGFP}$ mice polarized under Th1, Th17, and induced Treg conditions (A) without or (B) with addition of 10 nM 7α,25-OHC. Data is representative for three independent experiments.

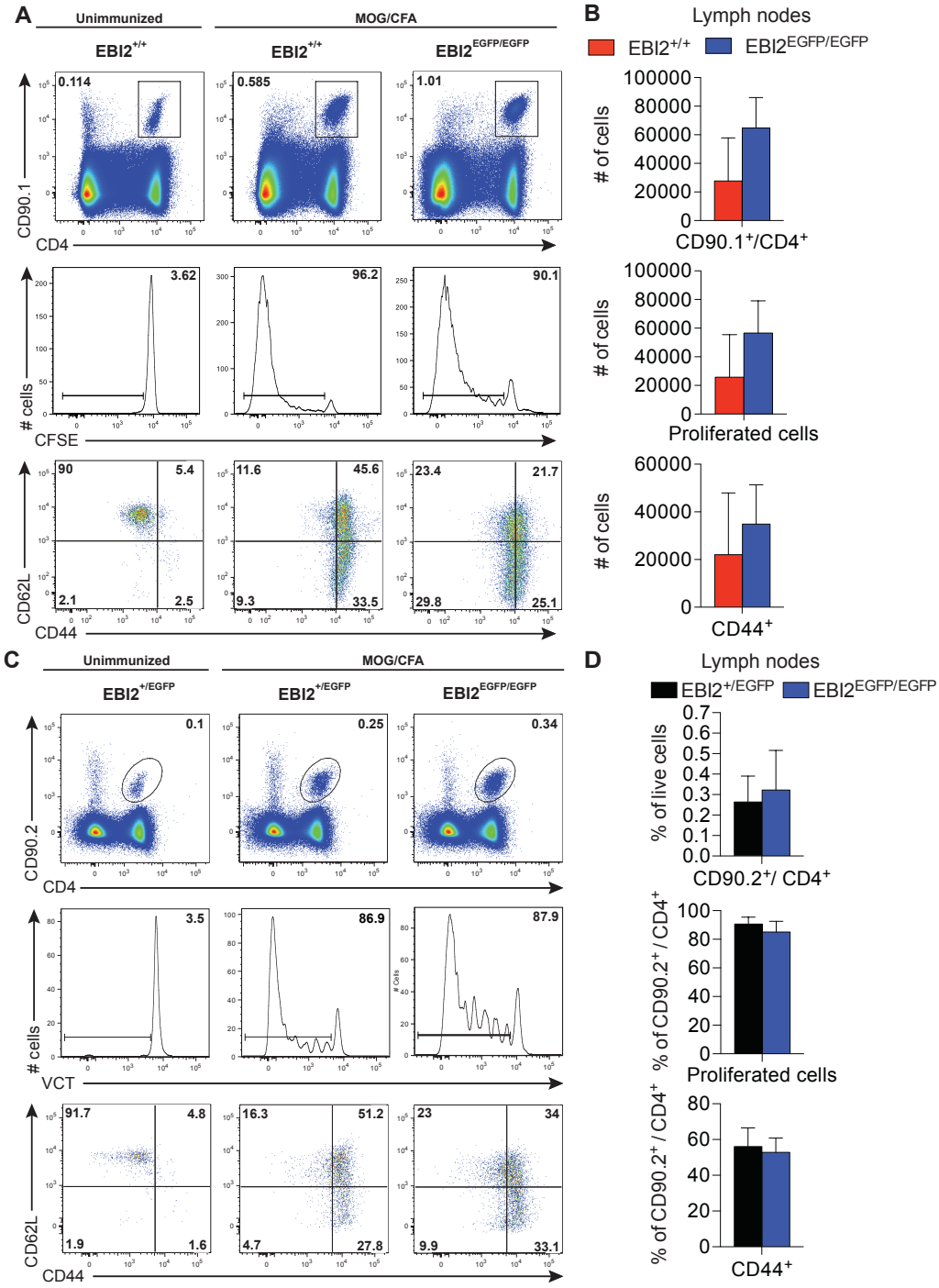

Figure S3. Related to Figure 3. (A-B) No differences in priming of T cells in EBI2 deficient mice. Purified $CD4^+$ T cells from 2D2 x Thy1.1 mice were labeled with CFSE and transferred into $EBI2^{EGFP/EGFP}$ mice or littermate controls. One day later, hosts were immunized with MOG/CFA or left untreated. Mice were sacrificed five days post immunization and analyzed by flow cytometry. Transferred T cells were gated as $CD90.2^-$, $CD90.2^+$, $CD4^+$ living cells and further analyzed for CFSE dilution and expression of CD62L and CD44. (A) Analysis of transferred T cells in the LNs of immunized or untreated hosts from indicated genotypes. (B) Statistical analysis of transferred T cells in the LNs of indicated hosts. Analysis of transferred T cells recovered from the spleen showed similar results (data not shown). Data is representative for two independent experiments (n=5). (C-D) No differences in priming of EBI2 deficient T cells in wt mice. Purified helper T cells from 2D2 x $EBI2^{+/EGFP}$ or 2D2 x $EBI2^{EGFP/EGFP}$ mice were labeled with VCT and transferred into congenic hosts. One day later hosts were immunized with MOG/CFA or left untreated. Mice were sacrificed five days post immunization and analyzed by flow cytometry. Transferred T cells were gated as $CD90.2^-$,

CD90.2$^+$, CD4$^+$ living cells and further analyzed for VCT dilution and expression of CD62L and CD44. (A) Analysis of transferred T cells from indicated genotypes in the LNs of immunized or untreated hosts. (D) Statistical analysis of transferred T cells from indicated genotypes in the LNs of immunized hosts. Data is representative for two independent experiments (n=3).

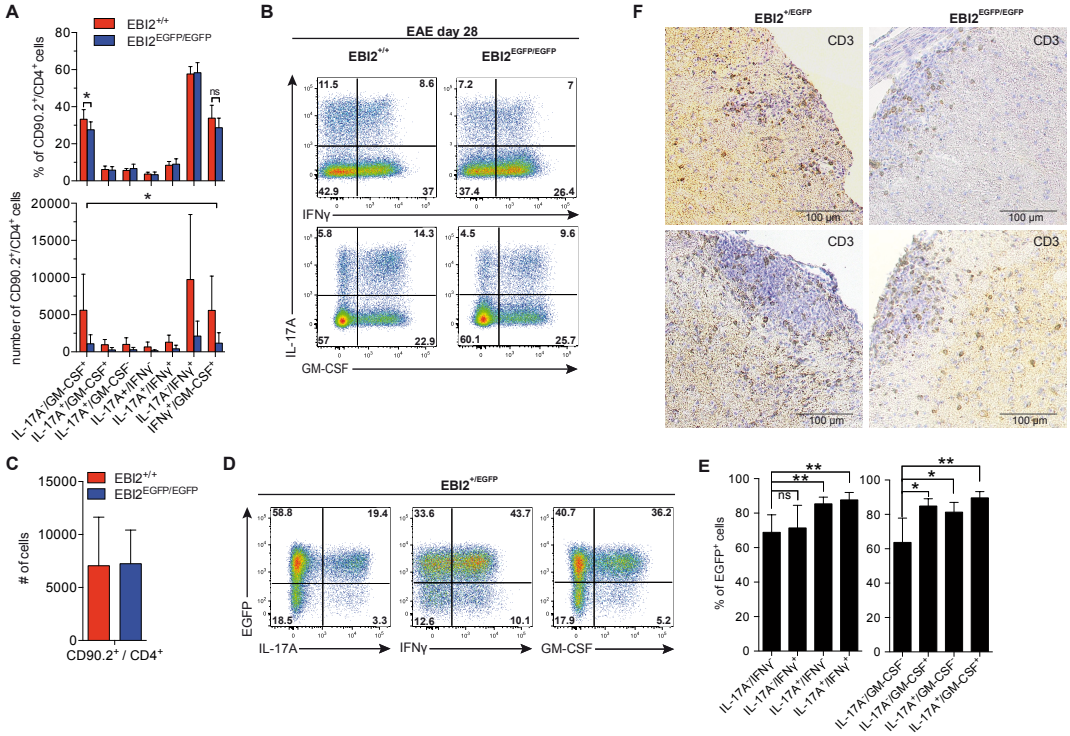

Figure S4. Related to Figure 4. Delayed onset of Th17 transfer EAE. (A) Cytokine expression of T cells early in transfer EAE at day 15. Upper graph shows the percentage of CNS infiltrating viable CD11b$^+$ / CD4$^+$/ CD90.2$^+$ T cells. Lower graph shows the number of the indicated cytokine secreting cells recovered from the CNS. Significance bar in lower graph indicates that all different T cell subsets differed significantly between WT and EBI2 deficient T cells. (B) Flow cytometric analysis of CD4$^+$ T cells within the CNS on day 28 post transfer. (C) Quantification of T helper cells within the CNS on day 28 post-transfer. (D) Analysis of EBI2-EGFP expression in cytokine expressing helper T cells in the CNS on day 28 post transfer. (E) Statistical analysis of EGFP$^+$ expression in cytokine secreting Th cells in the CNS. Data is representative for at least two independent experiments. (F) Histological analysis of CD3$^+$ T cells infiltrating the spinal cord (counterstained with hematoxylin) of RAG1 deficient mice on day 16 post transfer of expanded Th17 cells from the respective genotypes. EAE was at onset in mice, which had received EBI2 deficient transferred (data not shown). Upper row shows lesions of mice with low inflammation and lower row lesions from mice with stronger inflammation. Five mice per genotype of transferred T cells were histologically analyzed.

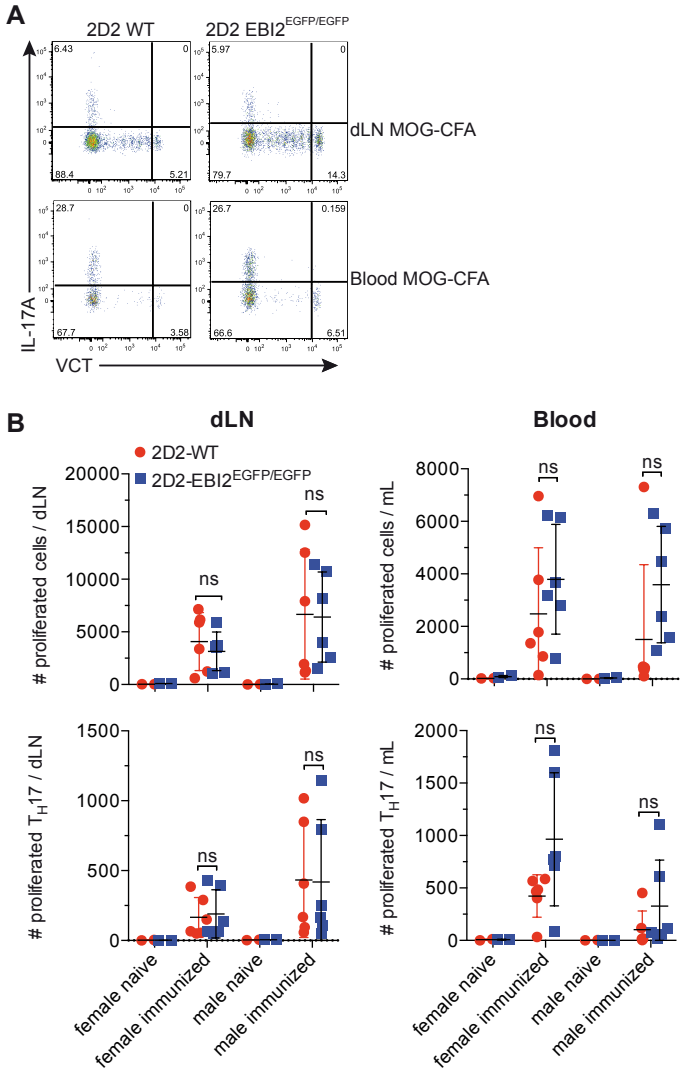

Figure S5. Related to Figure 5. (A) Flow cytometric analysis of proliferated (VCT low) viable (ViaDye low) transferred (CD45.2^{+}) CD90.1 positive (WT 2D2 T cells) or negative (EBI2 deficient 2D2 T cells) CD4^{+} T cells in dLN and blood on day 9 post transfer. (B) Quantification of proliferated T helper cells in dLN and blood on day 9 post transfer (upper panel) and proliferated Th17 cells in dLN and blood on day 9 post transfer.

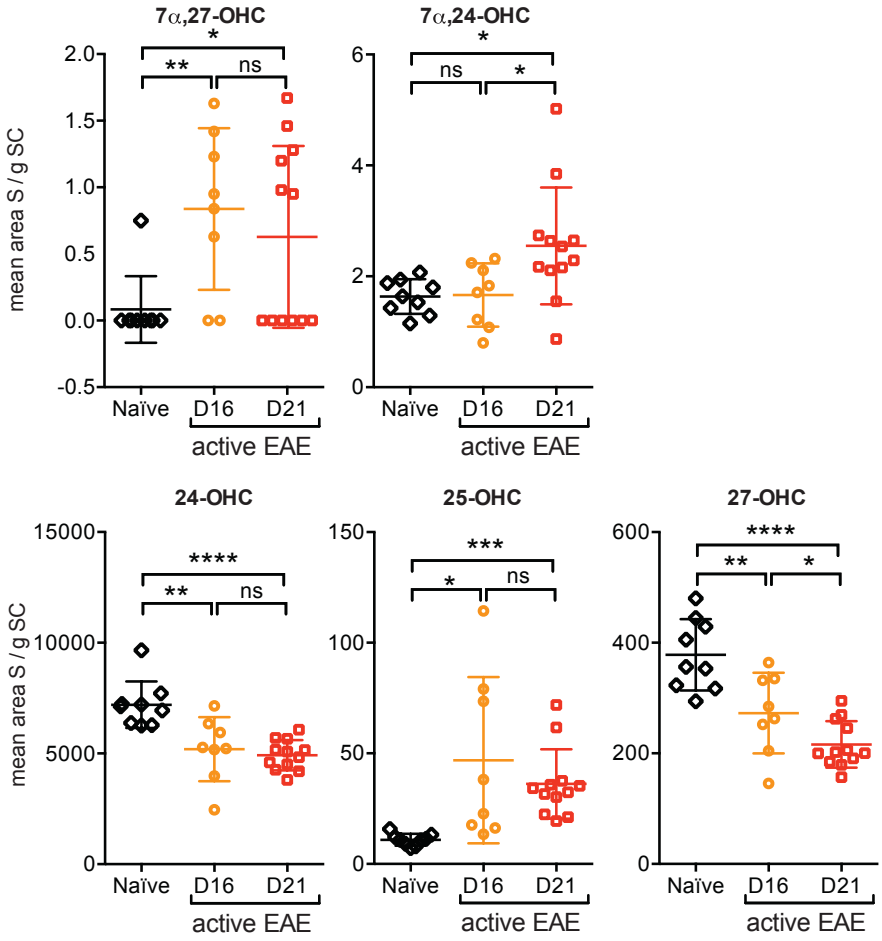

Figure S6. Related to Figure 6. Mono- and di-hydroxylated cholesterols in the spinal cord from naïve mice and mice with EAE. Spinal cords from naïve mice (n = 9), mice with EAE at day 16 post immunization (n = 8) and mice with EAE day 21 post immunization (n = 12) were extracted as described in the methods section. Subsequent uHPLC tandem massspectrometry was used to determine oxysterol levels. Data given is expressed as peak mean area in the chromatogram normalized to the spinal cord tissue weight used in the experiment (mean area S / gram spinal cord tissue).

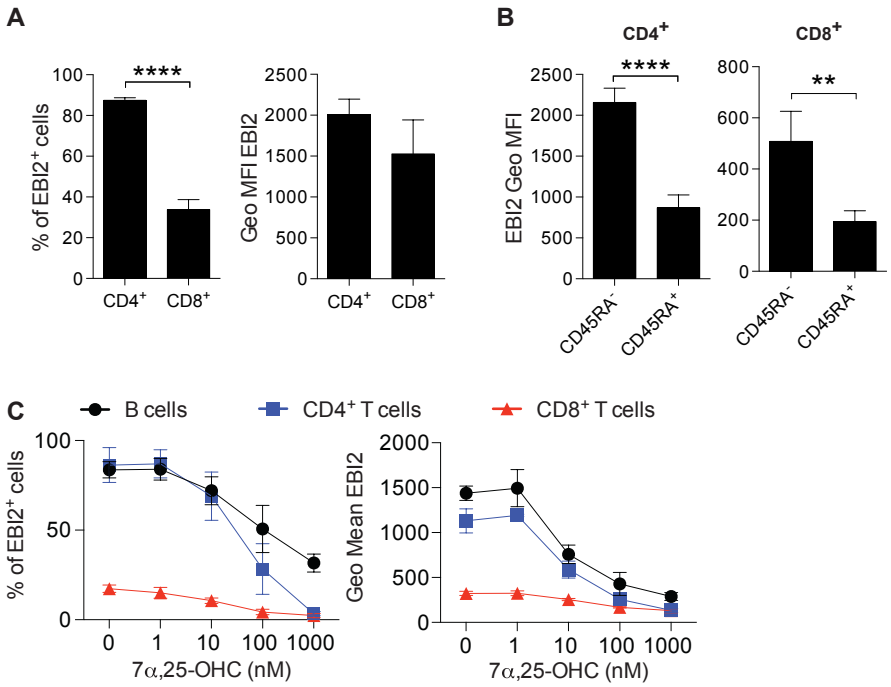

Figure S7. Related to Figure 7. EBI2 expression on human PBMCs. (A) Statistical analysis of EBI2$^+$ T cells and GeoMFI of EBI2 on respective subsets. (B) Statistical analysis of CD45RA$^+$ / CD45RA$^-$ T cells for EBI2 expression and GeoMFI of EBI2 on respective subsets. (C) Statistical analysis of EBI2 expression of indicated cells after incubation with indicated concentrations of 7α,25-OHC. Data is representative for at least two independent experiments with n=5.

Supplemental Tables

	Genotype / mouse strain	Disease incidence	Mean Max.	Mean day of onset* (p value**)
Exp. 1	$EBI2^{+/+}$	100% (11/11)	3.3 ± 0.75	8.6 ± 0.5
	$EBI2^{+/EGFP}$	87.5% (7/8)	3.3 ± 1.5	10
	$EBI2^{EGFP/EGFP}$	88.9% (8/9)	3.2 ± 1.5	12.6 ± 1.4 (n.a.)
Exp. 2	$EBI2^{+/+}$	100% (8/8)	2.9 ± 0.6	8 (n.a.)
	$EBI2^{+/EGFP}$	87.5% (7/8)	3.4 ± 1.1	8 (n.a.)
	$EBI2^{EGFP/EGFP}$	100% (8/8)	3.5 ± 0.7	8 (n.a.)
Exp. 3	$EBI2^{+/+}$	100% (10/10)	2.9 ± 0.8	8 (n.a.)
	$EBI2^{-/-}$	87.5% (7/8)	3 ± 1.2	8.1 ± 0.4 (n.a.)

Table S1. Related to Figure 3. Active EAE
Table shows results of three individual EAE experiments. Experiment 3 was performed using $EBI2^{-/-}$ mice, which lack EGFP reporter. Data shows disease incidence as percent of total group size and mouse numbers. Mean maximum disease score and mean day of onset (mice with EAE score ≥ 1) are shown with standard deviation. N.a.: not applicable.

	Genotype / mouse strain	Disease incidence	Mean Max.	Mean day of onset* (p value**)
15 days: Exp. 1	$EBI2^{+/+}$	100% (10/10)	1.9 ± 1.2	n.a.
	$EBI2^{EGFP/EGFP}$	55.6 (5/9)	1.2 ± 0.5	n.a.
15 days: Exp. 2	$EBI2^{+/+}$	88.9 % (8/9)	1.8 ± 1.1	n.a.
	$EBI2^{EGFP/EGFP}$	11.1% (1/9)	0.5	n.a.
28 days: Exp. 1	$EBI2^{+/+}$	100% (4/4)	3.3 ± 1.2	19.2 ± 2.2 (0.021)
	$EBI2^{+/EGFP}$	100% (4/4)	3 ± 1.5	21 ± 0.7 (0.006)
	$EBI2^{EGFP/EGFP}$	75% (3/4)	4	24 ± 1 (n.a.)
28 days: Exp. 2	$EBI2^{+/+}$	100 % (7/7)	3.9 ± 0.7	17.8 ± 3 (0.026)
	$EBI2^{+/EGFP}$	83.4% (5/6)	4.3 ± 0.3	15.8 ± 2.9 (0.002)
	$EBI2^{EGFP/EGFP}$	100% (11/11)	4	21.4 ± 2.4 (n.a.)

Table S2. Related to Figure 4. Th17 Transfer EAE
Table shows results of four individual transfer EAE experiments, which were either run for 15 or 28 days. Data shows disease incidence as percent of total group size and mouse numbers. Mean maximum disease score and mean day of onset (mice with EAE score ≥ 1) are shown with standard deviation. P value was calculated for mean day of onset compared to $EBI2^{EGFP/EGFP}$ mice using unpaired two-tailed Students t-test.

Supplementary methods

Measurements of oxysterol tissue levels by ultra-high performance liquid chromatography and tandem mass spectrometry (UHPLC-MS/MS).
Oxysterol standards and internal standards were purchased from Avanti Polar Lipids: 25-OHC, 27-OHC, 24S-OHC, 25-OHC-d6, 24(R/S)-OHC-d7, 7α,25-OHC, 7α,27-OHC, 7α,24S-OHC, 7α,25-OHC-d6, 7α,27-OHC-d6, 7α,24(R/S)-OHC-d7. Butylated hydroxytoluene (BHT) was purchased from SAFC (Sigma). Frozen spinal cord sample were weighted and placed in a Tissue Tube bag (TT05, Covaris, Woburn, MA, USA) for homogenization using Cryoprep ^{TM}Covaris CP-02 (Covaris, Woburn, MA, USA) with 200 µM BHT and a mixture of deuterated internal standard compounds. After pulverization, the sample was transferred into a Covaris glass tube, 200 µl water was then added. After being sonicated using a focused ultrasonicator Covaris E220x (Covaris, Woburn, MA, USA), sample was transferred in a micro reaction vial (1 mL) and 750 µl Chloroform / MeOH (v/v 1/2) was added. The mixture was homogenized on a Vortex 10 min using high speed and centrifuged for 5 min, at 2600 RPM and +4°C. Supernatant was transferred into a 5 mL micro reaction vial and the bottom phase was then extracted again with 750 µl chloroform / MeOH (v/v 1/2). The new supernatant was pooled with the first one and 0.5 mL chloroform and 0.5 mL water as added. After shaking for 10 min, the mixture was centrifuged for 5 min at 2600 RPM and 4°C for phase separation. The upper aqueous phase was then again extracted using 1 mL chloroform and 1 mL methanol (the bottom phase was kept). After phase separation, the bottom phase was taken and added to the first one. The extracts were then dried under N_2 stream at 40°C. The residue was re-suspended in 100 µl EtOH / H2O and centrifuged on Filter Ultrafree (Merck Millipore, Cork, Ireland) at 12000 RCF at 4°C. 10 µl were injected for UHPLC-MS/MS analysis. A Nexera UHPLC system (Shimadzu, Japan) was coupled to a QTrap®6500 (ABSciex, Framingham, USA) mass spectrometer. Chromatographic separation was achieved using an Acquity UPLC® BEH C18 column (100 x 2.1 mm, particle size 1.7µm) with a VanGuard™ pre-column Acquity UPLC® BEH C18 (5 x 2.1 mm, particle size 1.7 µm) (Waters, Milford, MA, USA). For the separation of monohydroxylated cholesterols, the mobile phases were delivered at a flow of 600 µl and a column temperature of 55°C. Mobile phase A consisted of 5% MeOH in H_2O and 0.1% formic acid (FA), whereas phase B of MeOH / acetronitrile and 0.1% FA. The gradient program was composed of three isocratic steps: 0-6 min 65% B, 7 min 70 % B and 2 min 97 % B. For the separation of the dihydroxylated cholesterols, a 10 min linear gradient program from 73-97 % B was applied with a flow rate of 400 µl / min and a column temperature of 55°C. Mobile phase A consisted of 5% MeOH in H_2O and 0.1% FA whereas phase B of MeOH and 0.1% FA. The mass spectrometer was equipped with an electrospray ionization source. The instrument was operated in a positive ion mode. Following MS/MS transitions were applied for the detection of oxysterols: m/z 385→m/z 157 and m/z 383 → m/z 159 for the mono-hydroxylated cholesterols and m/z 383 → m/z 157 and m/z 383 → m/z 159 for dihydroxylated cholesterols.

Single cell RT-PCR analysis of *Gpr183* expression
For single cell expression analysis, LN of healthy mice or mice at disease peak of MOG_{35-55}-induced active EAE were dissected, minced, filtered, and FACS sorted for CD4 expression. To isolate immune cells from spinal cords, an additional gradient centrifugation (Percoll) was performed before FACS sorting. To enrich regulatory T cells, in some cases cells from naïve or MOG/CFA immunized FoxP3-GFP reporter mice (Haribhai et al., 2007) were used. After FACS sorting, cells were loaded onto the microfluidic-C1 Single-Cell Auto Prep System (Fluidigm) followed by RNA isolation and cDNA synthesis. cDNAs derived from chambers containing no cell or more than one cell were excluded from further analysis. Quantitative PCR for *Gpr183* in single cell cDNAs was performed on a 96.96 Dynamic Array IFC with a BioMark system (Fluidigm) using Sso-Fast EvaGreen Supermix low ROX (BioRad, Hercules, CA, USA) and the primer pair *Gpr183*: 5'- AAACACGGACTGCCACAAC-3'/5' - TTGCCAGTGGGGTAGTGAAA-3'. Only single cell cDNAs negative for lineage markers *Cd8* ($CD8^+$ T cells), *Cd19* (B cells), *Ly6g* (neutrophils), *Cdh5* (endothelial cells), Myh11 (smooth muscle cells) were included into statistical analyses.

Human tissue samples and immunohistochemistry
We retrospectively investigated 5 brain biopsies from 5 MS patients. None of the study authors was involved in decision-making with respect to biopsy. All lesions fulfilled the generally accepted criteria for the diagnosis of multiple sclerosis (Prineas, 1985; Allen, 1991; Lassmann et al., 1998). The study

was approved by the Ethics Committee of the University of Münster. Tissue specimens were fixed in 4 % paraformaldehyde and embedded in paraffin. Tissue samples were cut in 4 µm thick sections that were stained with haematoxylin and eosin and Luxol-fast blue. Immunohistochemical staining was performed with an avidin-biotin technique using an automated staining device (DakoLink 48). The primary antibodies were rabbit anti-CD3 (Dako), mouse anti-EBI2 (1:500) clone 57C9B51C9 (Novartis). For double stainings, sections were incubated with the appropriate primary antibodies followed by secondary antibodies conjugated to Cy3 (Jackson Immunoresearch Laboratories) or Alexa488 (1:200) (Jackson ImmunoResearch Laboratories) conjugated antibodies and counterstained with DAPI (1: 5000) (Invitrogen). All images were taken on an Olympus fluorescent microscope. Mouse immunohistochemistry was performed as recently described (Klotz et al., 2016).

Supplementary References

Allen IV (1991). Pathology of multiple sclerosis. In: Matthews WB. McAlpine's Multiple Sclerosis. Edinburgh: Churchill Livingstone, 341-378.

Haribhai, D., Lin, W., Relland, L.M., Truong, N., Williams, C.B., and Chatila, T.A. (2007). Regulatory T cells dynamically control the primary immune response to foreign antigen. J Immunol *178*, 2961-2972.

Klotz, L., Kuzmanov, I., Hucke, S., Gross, C.C., Posevitz, V., Dreykluft, A., Schulte-Mecklenbeck, A., Janoschka, C., Lindner, M., Herold, M.*, et al.* (2016). B7-H1 shapes T-cell-mediated brain endothelial cell dysfunction and regional encephalitogenicity in spontaneous CNS autoimmunity. Proc Natl Acad Sci U S A *113*, E6182-E6191.

Prineas JW (1985). The neuropathology of multiple sclerosis. In: Koetsier JC. Demyelinating Diseases. Amsterdam: Elsevier Science Publishers, 213-257.